International Journal of Nanomedicine

Dovepress
open access to scientific and medical research

Open Access Full Text Article

ORIGINAL RESEARCH

Intravenously delivered graphene nanosheets and multiwalled carbon nanotubes induce site-specific Th2 inflammatory responses via the IL-33/ST2 axis

This article was published in the following Dove Press journal:
International Journal of Nanomedicine
2 May 2013
Number of times this article has been viewed

Xiaojia Wang[1]
Ramakrishna Podila[1]
Jonathan H Shannahan[1]
Apparao M Rao[2]
Jared M Brown[1]

[1]Department of Pharmacology and Toxicology, Brody School of Medicine, East Carolina University, Greenville, NC, USA; [2]Department of Physics and Astronomy, Clemson University, Clemson, SC, USA

Abstract: Carbon-based nanomaterials (CBN), such as graphene nanosheets (GNS) and multiwalled carbon nanotubes (MWCNT), have been proposed for potential nanomedicine applications such as biomedical devices and carriers for drug delivery. However, our current understanding regarding the systemic toxicity of these CBN through intravenous (iv) injection is limited. In this study, we compare the immune response resulting from GNS and MWCNT exposure. We hypothesize that iv administration of GNS and MWCNT would result in divergent systemic inflammatory responses due to physicochemical differences between these two CBN. In the lungs of C57BL/6 mice, GNS actuate a Th2 immune response 1 day following iv administration, which consists of neutrophilic influx and a significant increase in interleukin (IL)-5, IL-13, IL-33, and its soluble receptor (sST2) in the bronchoalveolar lavage fluid. MWCNT elicited a significant increase in the messenger ribonucleic acid expression of cytokines in the spleen including IL-4 and IL-33, which are associated with an increase in splenic cell differentiation (CD)4$^+$ and CD8$^+$ T-cells in C57BL/6 mice following iv injection. The observed Th2 responses in both the lung and spleen are absent in ST2$^{-/-}$ mice administrated GNS or MWCNT, suggesting a critical role for IL-33. In conclusion, the use of GNS or MWCNT as nanocarriers for drug delivery may result in Th2 immune responses that are mediated through the IL-33/ST2 axis and therefore may promote adverse allergic reactions.

Keywords: IL-33, ST2, graphene nanosheets, multiwalled carbon nanotubes, Th2 immune responses

Introduction

The development of diverse nanomaterials has added a new dimension to the rapidly expanding field of nanotechnology. The potential applications of nanomaterials range widely from biomedicine to mechanical engineering. One major biomedical application of nanomaterials is their usage in nanomedicine as diagnostic and therapeutic tools.[1,2] The advantage of utilizing nanomaterials as drug delivery systems is their capability of penetrating normally intact physiologic barriers and reaching a variety of molecular targets due to their size.[3–7] Currently, our understanding and knowledge regarding the potential toxicity and adverse health effects resulting from exposures to nanomaterials is insufficient. Unintentional or intentional exposure to nanomaterials may induce immunotoxicity resulting in detrimental effects to immune function. In vivo studies have demonstrated that nanoparticles are capable of promoting inflammation or suppressing immune functions.[8–10] This nanoparticle-induced inflammatory response

Correspondence: Jared M Brown
Department of Pharmacology and Toxicology; Brody School of Medicine, East Carolina University, 6W-33 Brody Building, Greenville, NC 27834 USA
Tel +1 252 744 2108
Fax +1 252 744 3203
Email brownja@ecu.edu

may have an impact on immune defense, and the Th1/Th2 balance.[3] Limited studies, however, have been focused on immune effects in vivo through iv injection, even though this will be a primary route for delivering nanomedicine.[11]

Carbon-based nanomaterials (CBN) represent a highly applicable subset of nanoparticles that have garnered considerable interest as carriers for a variety of therapeutic agents. CBN consist of many different forms, including fullerenes, single- and multiwalled carbon nanotubes (SWCNT and MWCNT, respectively), and graphene nanosheets (GNS). MWCNT exist with a one-dimensional structure, whereas GNS have a two-dimensional lattice causing them to have markedly dissimilar geometric shapes, which may influence their therapeutic potential through altering their biodistribution and/or toxicity. In addition to differences in shape, MWCNT and GNS are synthesized by different methods resulting in diverse physicochemical properties and catalyst impurities. Specifically, the MWCNT used in this study were ~25 nm in diameter, with a surface area of ~113 m^2/g and ~5 wt% Fe catalyst. Two types of GNS were also evaluated in this study including GNS (2) with a thickness of ~2 nm, and GNS (5) with a ~5 nm thickness. Both types of GNS, however, exist with a theoretical surface area of ~2630 m^2/g and have no metal catalyst present. This large surface area-to-volume ratio of GNS provides an ideal platform for use as a drug delivery system in nanomedicine, but it may also disrupt immune function.

Recently, we have demonstrated that pulmonary instillation of MWCNT in mice induces interleukin (IL)-33 production and may function as an "alarmin" in response to nanomaterial exposure.[12,13] IL-33 is a novel member of the IL-1 family of cytokines that includes IL-1α/β, IL-1Ra, and IL-18.[14] Interaction of IL-33 with its receptor, ST2, promotes a variety of actions from various cell types, including basophils, mast cells, macrophages, and Th2 cells.[15,16] ST2 is a member of the IL-1 receptor (IL-1R) family with two isoforms: a membrane-bound receptor (ST2) and a soluble receptor (sST2).[17] SST2 can function as a decoy receptor binding IL-33 thereby inhibiting signaling through the membrane-bound receptor, ST2.[18] In addition, the IL-33/ST2 axis is involved in the promotion and maintenance of $CD4^+$ Th2-type allergic inflammation by stimulating the production of IL-5 and IL-13.[14] Recently, ST2 expression on cytotoxic ($CD8^+$) T cells has been found under certain in vitro culture conditions.[19]

In this study, we hypothesized that intravenous (iv) administration of GNS and MWCNT would result in divergent systemic inflammatory responses due to physicochemical differences between these two CBN. Furthermore, we hypothesize that the underlying mechanism responsible for these immune effects by CBN is through the activation of the IL-33/ST2 axis. To verify this hypothesis, we intravenously injected C57BL/6 and ST2 knockout ($ST2^{-/-}$) mice with MWCNT, GNS (2), or GNS (5). In general, C57BL/6 mice injected with CBN exhibited site-specific inflammatory responses with increased IL-33 levels in the lung following GNS injection, while MWCNT injected mice demonstrated elevation of Th2 cytokines and increases in the number of $CD4^+$ and $CD8^+$ T-cells in the spleen. Furthermore, we determined the importance of the IL-33/ST2 axis in mediating these effects by demonstrating an absence of these effects in mice lacking the ST2 receptor when exposed to both forms of CBNs.

Materials and methods

Graphene synthesis

GNS (2) and GNS (5) were synthesized using the solvent exfoliation method. Briefly, for solvent exfoliation of graphene, bulk graphite (~1 g) was dispersed in 100 mL of N-methyl-2-pyrrolidinone and sonicated using a 1/8 inch tip sonicator (Branson 250; Branson Ultrasonics Corporation, Danbury, CT, USA) at 100 W for 2 hours. The resulting dispersion was filtered through a 0.45 μm nylon filter to obtain GNS (5). For GNS (2), the solution was subjected to a second sonication step for 6 hours and centrifuged at 500 rpm for 45 minutes. The supernatant was vacuum filtered using a 0.45 μm nylon filter. Finally, the filtered powder was washed several times using deionized water to remove residual N-methyl-2-pyrrolidinone.

Graphene and MWCNT characterization

Commercial grade NWCNT were generously provided by NanoTechLabs, Inc (Yadkinville, NC, USA). The CBN used in this study were characterized using a Hitachi H-7600 electron microscope (Hitachi Ltd, Tokyo, Japan). A Dilor XY triple-grating spectrometer with Ar+ excitation at 514.5 nm was used for Raman spectroscopy. The hydrodynamic size was characterized using dynamic light scattering (Nanosizer S90; Malvern Instruments, Malvern, UK). The zeta potential was determined using a zeta potential device (Zeta ZS; Malvern Instruments). For the light scattering measurement (dynamic light scattering and zeta potential), we have suspended the materials in the media consisting of 0.6 mg/mL mouse serum albumin (MSA) and 0.01 mg/mL of 1,2-dipalmitoyl-sn-glycero-3-phosphocholine (DPPC) in sterile phosphate buffered saline.

Animals

Male C57BL/6 mice were acquired from The Jackson Laboratory (Bar Harbor, ME, USA) at 8–10 weeks of age. ST2$^{-/-}$ mice were generously provided by Dr Robert B Fick (Merck, Inc), and breeding colonies were maintained at East Carolina University. All animal procedures were conducted in accordance with the National Institutes of Health guidelines and approved by the East Carolina University Institutional Animal Care and Use Committee. All animals were treated humanely and with regard for alleviation of suffering.

Nanomaterials were suspended in dispersion media consisting of 0.6 mg/mL MSA and 0.01 mg/mL of DPPC in sterile phosphate buffered saline, as previously described,[20] and dispersed by cup horn sonication to ensure sterility. The preparation of nanomaterials dispersions in a dispersion medium containing MSA and DPPC ensured stability of the formulations. C57BL/6 and ST2$^{-/-}$ mice were randomly assigned to four treatment groups (4–8 mice/group), which included vehicle (dispersion media), MWCNTs, GNS (2), or GNS (5). Mice received a single dose of CBN by tail vein injection at 1 mg/kg body weight of MWCNTs, GNS (2), GNS (5), or dispersion media as vehicle control. For example, a 25 g mouse would receive 200 µL (body weight × 8) of 0.125 mg/mL nanomaterial via injection resulting in a dose of 1 mg/kg. Mice were sacrificed at day 1 or 7 postinjection to follow the development of systemic immune responses.

BAL and cell differential counts

One or 7 days postinjection, all mice were anesthetized and underwent in situ bronchoalveolar lavage (BAL), as previously reported.[12] Briefly, BAL was performed on the right lung of each mouse four separate times each with an individual volume based on body weight (26.25 mL/kg of body weight) of Hanks balanced salt solution. The first aliquot of BAL fluid (BALF) was collected separately for cytokine analysis, while aliquots 2–4 were pooled. All BALF was centrifuged at 1000 × g for 10 minutes at 4°C. Total cells from lavages were pooled and counted using Cellometer® Auto X4 Cell Counters (Nexcelom Bioscience, LLC, Lawrence, MA, USA). 20,000 cells were centrifuged using Cytospin 4 (Shandon Scientific Ltd, Cheshire, UK) and stained with a three-step hematology stain (Richard-Allan Scientific, Kalamazoo, MI, USA). Cell differential counts were determined by morphology with evaluation of 300 cells/slide.

ELISA

Samples from individual animals were run in duplicate for the quantification of BALF cytokine (IL-5, IL-13, IL-33, and sST2) levels and serum IL-5 levels using DuoSet ELISA kits (R&D Systems, Minneapolis, MN, USA) in accordance with the manufacturer's instructions. Values are reported as pg/mL ± standard error of the mean.

Spleen weight and spleen cell isolation

Following BAL, spleens were removed from animals and weighed. Single-cell suspension of a quarter spleen were obtained by using the gentleMACS™ Dissociator (Miltenyi Biotec, Inc, Auburn, CA, USA) according to the manufacturer's recommendations. Red blood cells were removed using a red blood cell lysis buffer (eBioscience, San Diego, CA, USA). Splenocytes were resuspended in a final volume of 5 mL of MACs buffer (Miltenyi Biotec, Inc). Quantification of total splenocytes and total live cells was performed by fluorescence assays for deoxyribonucleic acid (DNA) staining dye (Acridine orange and propidium iodide [Invitrogen, Eugene, OR, USA]) using Cellometer® Auto X4 Cell Counters (Nexcelom Bioscience LLC). A total of 20,000 live splenocytes were centrifuged using Cytospin 4 (Shandon Scientific Ltd) and stained with a three-step hematology stain (Richard-Allan Scientific). Spleen cell differential counts were determined by morphology with evaluation of 300 cells/slide.

Flow cytometry

Isolated cell suspensions (1×10^6 cells/sample) from spleens were preincubated with anti-CD16/32 (AbD Serotec, Kidlington, UK) on ice for 10 minutes prior to incubation. Fluorescein isothiocyanate-conjugated antimouse CD4 (L3T4) and PerCP-Cy5.5 conjugated antimouse CD8 (Ly-2) antibodies obtained from eBioscience were used to stain splenocytes at room temperature for 30 minutes in the dark. Flow cytometric analysis of the stained splenocytes was performed with an Accuri C6 flow cytometer (BD Accuri™ Cytometers; BD Biosciences, Ann Arbor, MI, USA).

Histopathology

The left lung and spleen were perfused with 10% zinc formalin fixative and allowed to fix for 24 hours prior to processing. Lung and spleen tissue were processed and embedded in paraffin, and 5 µM sections were mounted on slides. Sections were stained with hematoxylin and eosin to detect inflammatory and morphological changes, as well as nanoparticle deposition. The size of CBN aggregates in the lung was evaluated by measuring the length at the longest axis (L) as well as the perpendicular axis (P). The

number of nanoparticle agglomerates was determined from representative lung sections. Spleen sections were blinded and evaluated by certified pathologists from Experimental Pathology Laboratories (EPL, Inc, Sterling, VA, USA).

Immunofluorescence

Unstained histological spleen sections from C57BL/6 mice were used for immunofluorescence detection of IL-33 protein expression, as previously described.[13] Spleen sections were deparaffinized and were blocked in blocking buffer (5% filtered fetal bovine serum in Tris buffer saline [TBS] with 0.2% Tween) for 2 hours, after which the IL-33 primary antibody was applied at 1:100 (Novus Biologicals, LLC, Littleton, CO, USA) for 48 hours at 4°C. Sections were washed one time with TBS and two times with blocking buffer, and then incubated in a DyLight® 550 conjugated secondary antibody at 1:100 (Abcam plc, Cambridge, MA, USA) for 2 hours at room temperature. Following additional washes in TBS with 0.1% Triton X, sections were coverslipped using Prolong gold antifade containing a 4′,6-diamidino-2-phenylindole, dilactate (DAPI) stain (Molecular Probes®; Molecular Probes, Inc, Eugene, OR, USA). Dry sections were imaged using DAPI and TRITC filters for nuclear- and IL-33-specific staining.

Quantitative Real-Time PCR

Total ribonucleic acid (RNA) from a spleen biopsy was isolated using a Direct-zol™ RNA MiniPrep (Zymo Research Corporation, Irvine, CA, USA) according to the manufacturer's recommendations. Total RNA (1 μg) was reverse-transcribed to complementary DNA (cDNA) using an iScript™ cDNA Synthesis Kit (Bio-Rad Laboratories, Inc, Hercules, CA, USA). Quantitative real-time polymerase chain reaction (PCR) was performed using SsoAdvanced™ SYBR® Green Supermix (Bio-Rad Laboratories, Inc) and QuantiTect primer assays (QIAGEN, Valencia, CA, USA). An Applied Biosystems StepOnePlus Real-Time PCR System (Life Technologies, Carlsbad, CA, USA) was used to obtain cycle threshold (Ct) values for target and internal reference cDNA levels. Target cDNA levels were normalized to glyceraldehydes 3-phosphate dehydrogenase, an internal reference, using the equation $2^{-[\Delta Ct]}$, where ΔCt is defined as $Ct_{target} - Ct_{internal\ reference}$. Values shown are the average of four independent experiments.

Statistical analyses

All data are presented as the mean ± standard error of the mean, and were analyzed by one-way analysis of variance (ANOVA) or two-way ANOVA, with differences between groups assessed using Bonferroni post hoc tests. Graphs and analyses were performed using GraphPad Prism 5 software (GraphPad Software, Inc, La Jolla, CA, USA). Differences were considered statistically significant at $P < 0.05$.

Results

Characterization and detection of GNS and MWCNT

GNS and MWCNT were characterized using transmission electron microscopy and Raman spectroscopy. As shown in Figure 1, GNS (2) and GNS (5) exhibited flake-like morphology with an area ~4 μm^2 and 25 μm^2, while MWCNTs exhibited tubular morphology with a length of ~10–20 microns and diameter of ~20–30 nm. The Raman spectra exhibited strong graphitic or G-band (~1590 cm^{-1}), consistent with previous studies.[12,13] We used the G-band signal (Figure 1D, as well as Figures S1 and S2 in the supplementary materials) in the Raman spectrum to confirm whether the black particulates found in the lung and spleen were GNS and MWCNT, concurring with previous studies.[21,22] As shown in Table 1, the hydrodynamic sizes of MWCNT, GNS (2), and GNS (5) are 792.70 ± 20.30, 823.85 ± 25.60, and 6600.00 ± 178.40 nm, respectively. The MWCNT suspension displayed a zeta potential of −20.79 ± 1.52 mV, whereas the zeta potential of GNS (2) suspension was −33.17 ± 2.04 mV and the zeta potential of GNS (5) suspension was −28.56 ± 3.30 mV, suggesting a stable colloidal state of the nanomaterials.

Intravenous administration of GNS promotes a Th2 response in the lung via the IL-33/ST2 axis

We have recently reported that IL-33 drives both pulmonary and cardiovascular toxicity of MWCNT in C57BL/6 mice following pulmonary instillation; therefore, we hypothesized that iv delivery of CBN may elicit similar responses resulting in systemic toxicity.[12,13] To investigate whether iv injection of CBN activates the IL-33/ST2 axis, we first examined protein levels of IL-33 and sST2 in BALF. At 1 day postinjection, C57BL/6 mice injected with 1 mg/kg of GNS (2) demonstrated a significant increase in both IL-33 and sST2 levels in BALF compared to vehicle-injected mice (Figure 2A and B). IL-33 was also significantly increased at 1 day following a 1 mg/kg injection of GNS

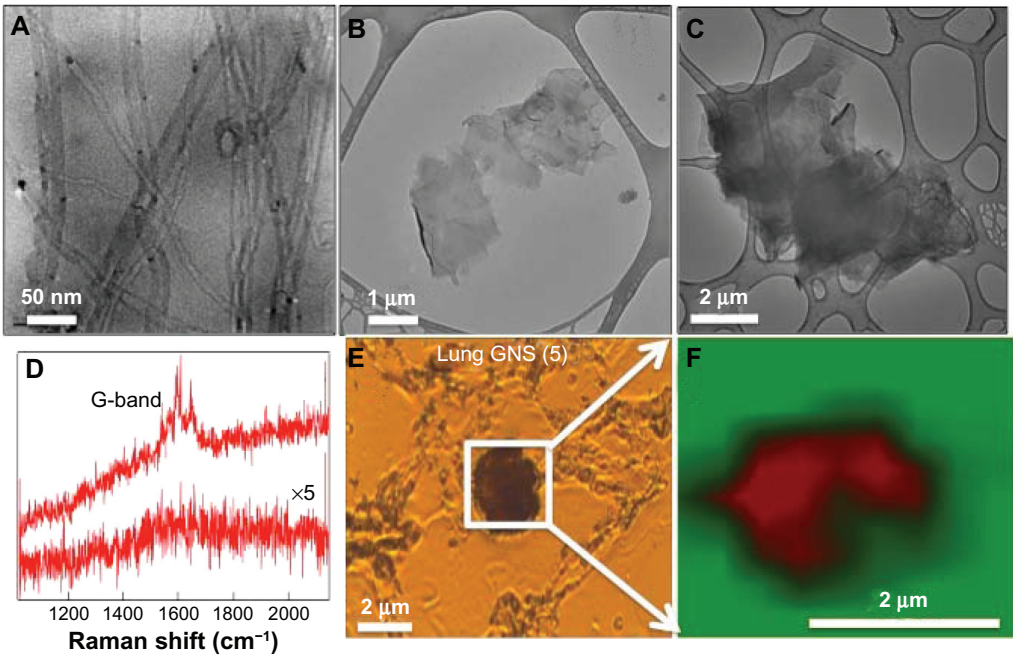

Figure 1 Characterization of carbon-based nanomaterials. Transmission electron micrographs for (**A**) MWCNT, (**B**) GNS (2), and (**C**) GNS (5). (**D**) Raman spectrum for the carbon-based nanomaterials (top spectrum) exhibits a strong graphitic or G-band ~1590 cm^{-1} while the animal tissue (bottom spectrum) shows no such signature. (**E**) Optical micrograph of a typical lung section exposed to GNS (5). (**F**) Raman G-band map of the boxed area in (**E**) shows that that the black spots seen in the optical micrograph are indeed carbon nanomaterials.

Notes: In the Raman micrograph, red and green colored areas represent a high and no intensities for G-band, respectively. Similar Raman confirmation was obtained for other lung and spleen sections exposed to MWCNT, GNS (2), and GNS (5) (see Supplementary materials for further details).

Abbreviations: MWCNT, multiwalled carbon nanotubes; GNS, graphene nanosheets.

(5) in comparison to vehicle-injected animals. In contrast to our previous studies that demonstrated increased IL-33 following pulmonary instillation of MWCNT,[12,13] IL-33 did not increase within the BALF following iv injection of MWCNT.

Given that IL-33 induces the release of Th2 cytokines through the ST2 receptor in a variety of immune cells, we examined protein levels of IL-5, IL-13, and interferon (IFN)-γ in BALF of C57BL/6 and $ST2^{-/-}$ mice 1 or 7 days following a single injection of CBN. GNS (2)-injected C57BL/6 mice that had increased levels of IL-33 in BALF (Figure 2) also displayed increases in both IL-5 and IL-13 at 1 day following injection (Figure 3A and B). Elevation of these Th2 cytokines was not observed in the BALF of $ST2^{-/-}$ mice at 1 day following CBN injection compared to vehicle (Figure 3A and B). A comparison between strains revealed a significant decrease in IL-5 and IL-13 between the C57BL/6 mice and the $ST2^{-/-}$ mice at 1 day following the injection of GNS (2). However, no statistically significant changes in IL-5 and IL-13 production in BALF of C57BL/6 and $ST2^{-/-}$ mice were found 7 days following CBN injection (Figure S3A and B). IFN-γ levels were not detectable in the BALF (data not shown).

To determine if an increase in IL-33 in BALF following CBN injection elicits a pulmonary inflammatory cell response, we examined differential cell counts from the BAL of C57BL/6 and $ST2^{-/-}$ mice at 1 or 7 days postinjection. A significant elevation in neutrophils was observed in C57BL/6 mice at 1 day postinjection of 1 mg/kg GNS (2) compared to controls (Table 2). Eosinophils and lymphocytes were also increased in C57BL/6 mice 7 days postinjection of 1 mg/kg GNS (5) (Table 2). However, no significant differences in differential

Table 1 Characterization of carbon-based nanomaterials in suspension

Nanomaterial	Descriptive dimensions	Zeta potential (mV)	Hydrodynamic size (nm)
MWCNT	25 ± 5 nm diameter, 15 ± 5 µm length	−20.79 ± 1.52	792.70 ± 20.30
GNS (2)	2 ± 1 nm thick, 4 ± 1 $µm^2$ area	−33.17 ± 2.04	823.85 ± 25.60
GNS (5)	5 ± 1 nm thick, 25 ± 5 $µm^2$ area	−28.56 ± 3.30	6600.00 ± 178.4

Abbreviations: MWCNT, multiwalled carbon nanotubes; GNS, graphene nanosheets.

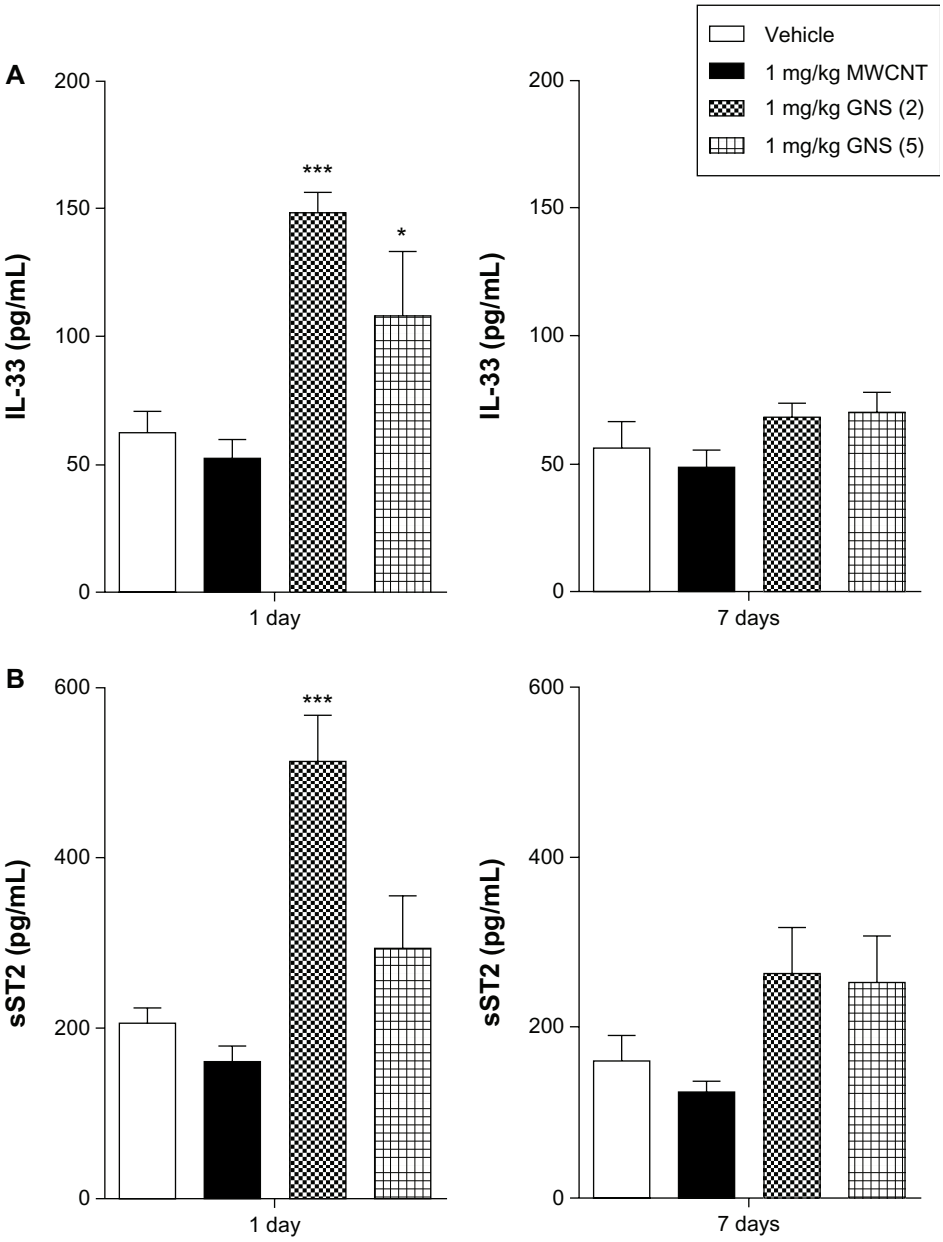

Figure 2 IL-33 and sST2 production in BALF of C57BL/6 mice 1 or 7 days postinjection with MWCNT, GNS (2), or GNS (5). IL-33 and sST2 levels were determined by ELISA in BALF of C57BL/6 mice intravenously injected with vehicle or 1 mg/kg of MWCNT, GNS (2), or GNS (5). (**A**) IL-33 and (**B**) its soluble receptor sST2 protein levels 1 or 7 days following injection of CBNs.

Notes: Values are expressed as the mean ± SEM (n = 4–8 per group). *$P < 0.05$ and ***$P < 0.001$ compared to vehicle controls.

Abbreviations: IL, interleukin; sST2, soluble receptor; BALF, bronchoalveolar lavage fluid; MWCNT, multiwalled carbon nanotubes; GNS, graphene nanosheets; ELISA, enzyme-linked immunosorbent assay; CBNs, carbon-based nanomaterials; SEM, standard error of the mean; n, number.

cell counts were found in the BALF of ST2$^{-/-}$ mice (Table 2). Histological evaluation of lung sections confirmed the altered inflammatory cell profile in C57BL/6 mice (Figure 4). At 1 day postinjection, the majority of MWCNT aggregates were found in the pulmonary capillary lumen of C57BL/6 (Figure 4B; yellow arrow) and ST2$^{-/-}$ mice (Figure S4B; yellow arrow), while both types of GNS translocated from the capillary into the alveolar air space (Figure 4C, D, G, and H, as well as Figures S4C, D, G, and H). Lastly, the size of the MWCNT and GNS aggregates in the lung decreased in size between 1 and 7 days (Table S1).

Intravenous administration of MWCNT elicits a CD4$^+$ Th2 response and CD8$^+$ response in the spleen dependent on the IL-33/ST2 pathway

We evaluated Th1/Th2 inflammatory responses in the spleen of C57BL/6 and ST2$^{-/-}$ mice by measuring messenger RNA

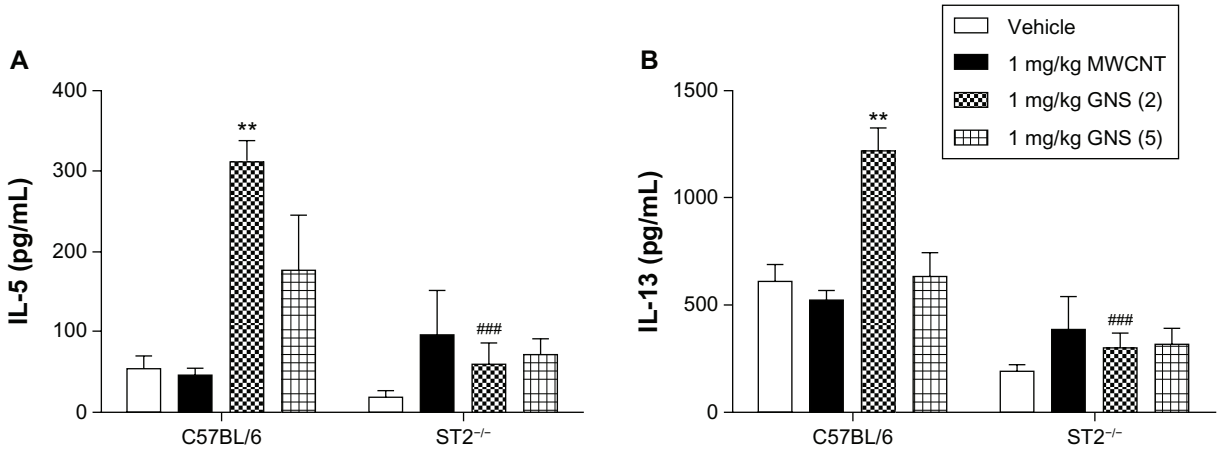

Figure 3 Th2 cytokine production in BALF of C57BL/6 and ST2$^{-/-}$ mice 1 day postinjection with MWCNT, GNS (2), or GNS (5). Production of the Th2 cytokines, (**A**) IL-5 and (**B**) IL-13, were measured by ELISA in BALF from lungs of C57BL/6 and ST2$^{-/-}$ mice at 1 day following injection with vehicle or 1 mg/kg of MWCNT, GNS (2), or GNS (5).
Notes: Values are expressed as the mean ± SEM (n = 4–8 per group). $^{**}P < 0.01$ compared to strain-matched vehicle control; $^{###}P < 0.001$ compared to C57BL/6 injected with GNS (2).
Abbreviations: BALF, bronchoalveolar lavage fluid; MWCNT, multiwalled carbon nanotubes; GNS, graphene nanosheets; IL, interleukin; ELISA, enzyme-linked immunosorbent assay; SEM, standard error of the mean; n, number.

(mRNA) levels of IL-4, IL-5, IL-33 and IFN-γ. One day after iv injection of a single 1 mg/kg dose of MWCNT, a significant increase in IL-4 and IL-33 mRNA expression was observed in C57BL/6 mouse spleens (Figure 5A), whereas GNS injection did not result in any increase in cytokine mRNA expression. Significantly increased mRNA levels of IL-33 were observed in C57BL/6 mice 7 days following iv injection of 1 mg/kg MWCNT compared to controls (Figure 5B). Protein levels of IL-33 from CBN-injected groups was notably increased in the spleen and not colocalized to the nucleus (Figure 6). Although there was a trend toward increased IL-5 levels in the spleens of C57BL/6 mice, the difference between CBN treated and control mice did not reach significance (Figure 5A and B). A significant increase in the serum levels of IL-5 in C57BL/6 mice was found 1 day after injection of 1 mg/kg GNS (5) (10.65 ± 3.88 pg/mL) compared to vehicle (1.95 ± 0.88 pg/mL), while no other CBN exposures were different from controls (data not shown). In contrast to C57BL/6 mice, there were no significant differences in cytokine mRNA expression levels at 1 or 7 days postinjection of CBN in ST2$^{-/-}$ mice, further illustrating the importance of the IL-33/ST2 axis (Figure 5C and D).

To further elucidate the implications of the altered cytokine profile in the spleen following CBN delivery, we assessed the proliferation of CD4$^+$ and CD8$^+$ T lymphocytes by flow cytometry at 1 and 7 days in C57BL/6 and ST2$^{-/-}$ mice (Figure 6). The percentage of CD4$^+$ and CD8$^+$ T lymphocytes in the spleen was significantly increased in C57BL/6 mice 1 day following injection with 1 mg/kg MWCNT, but not GNS, compared to controls (Figure 7A and B). This increase in CD4$^+$ T lymphocytes remained elevated through 7 days following iv injection with MWCNT, whereas the percentage of CD8$^+$ T lymphocytes returned to control levels by 7 days (Figure 7C and D). This influence of CBN on lymphocyte populations was dependent on ST2 expression, as it was not observed in ST2$^{-/-}$ mice (Figure 7A–D). Differential spleen cell counts from all treatment groups did not demonstrate significant differences when compared to controls, except for the total cell count from the GNS (5) 1-day treatment (Table 3). There were, however, no discernible pathological differences in the spleens of CBN-exposed animals compared to controls. This was likely due to the high inflammatory cell composition of the spleen, thereby inhibiting our ability to detect subtle differences in inflammation by microscopy (data not shown).

Discussion

We have previously demonstrated that pulmonary instillation of MWCNT in C57BL/6 mice leads to a Th2-type immune response with increased numbers of inflammatory cells and increased Th2 cytokine levels in the lung.[12,13] Furthermore, we have demonstrated that these MWCNT-induced Th2 immune responses are mediated by mast cell activation in the pulmonary system through the IL-33/ST2 axis.[13] In our current study, we compared the systemic immune responses that were initiated following iv delivery of GNS and MWCNT. In C57BL/6 mice, iv administration of GNS and MWCNT resulted in the accumulation of CBN in the lung and spleen. In the lungs of C57BL/6 mice, the smaller sized GNS (GNS [2]) triggered an increase in IL-33 and sST2, resulting in a Th2 immune response consisting of neutrophilic influx and increases in IL-5 and IL-13. While delivery of MWCNT

Table 2 Effect of MWCNT and GNS on bronchoalveolar lavage cell populations in C57BL/6 and ST2$^{-/-}$ mice at 1 day or 7 days following intravenous injection

Strain	Time point	Treatment	Macrophages ($\times 10^3$ cells/mL)	Epithelial cells ($\times 10^3$ cells/mL)	Neutrophils ($\times 10^3$ cells/mL)	Eosinophils ($\times 10^3$ cells/mL)	Lymphocytes ($\times 10^3$ cells/mL)	Monocytes ($\times 10^3$ cells/mL)	Total cells ($\times 10^3$ cells/mL)
C57BL/6	1 day	Vehicle	149.42 ± 33.45	17.02 ± 10.13	0.33 ± 0.16	0	1.33 ± 0.62	0.52 ± 0.20	168.61 ± 42.73
		1 mg/kg MWCNT	194.14 ± 45.47	19.79 ± 5.74	1.24 ± 0.35	0.26 ± 0.26	3.48 ± 1.75	0.64 ± 0.17	219.55 ± 51.87
		1 mg/kg GNS (2)	195.87 ± 10.33	21.58 ± 3.55	5.44 ± 1.96***	0.20 ± 0.20	4.46 ± 1.05	1.71 ± 0.95	229.25 ± 12.40
		1 mg/kg GNS (5)	117.23 ± 16.55	9.63 ± 2.56	1.32 ± 0.22	0	3.80 ± 0.61	0.52 ± 0.33	132.50 ± 17.28
	7 days	Vehicle	144.67 ± 19.63	12.95 ± 3.42	0.21 ± 0.13	0.44 ± 0.23	1.12 ± 0.17	0	159.38 ± 22.23
		1 mg/kg MWCNT	159.49 ± 31.53	12.25 ± 2.63	1.84 ± 0.46	1.47 ± 0.32	5.02 ± 1.83	0.43 ± 0.25	180.50 ± 36.26
		1 mg/kg GNS (2)	149.91 ± 12.45	14.12 ± 2.42	1.02 ± 0.19	0.94 ± 0.79	3.42 ± 0.77	1.09 ± 0.46	170.50 ± 14.89
		1 mg/kg GNS (5)	164.39 ± 24.45	10.51 ± 1.72	2.28 ± 0.32	4.02 ± 1.05*	12.15 ± 3.47***	1.32 ± 0.43	194.67 ± 24.99
ST2$^{-/-}$	1 day	Vehicle	134.50 ± 11.71	10.76 ± 1.73	0.11 ± 0.11	0	0	0	145.38 ± 10.40
		1 mg/kg MWCNT	225.88 ± 54.35	6.06 ± 0.68	0.31 ± 0.31	0	0	0	232.25 ± 54.81
		1 mg/kg GNS (2)	139.39 ± 23.55	11.13 ± 3.40	0.17 ± 0.17	0	0.20 ± 0.12	0	150.88 ± 25.15
		1 mg/kg GNS (5)	186.65 ± 38.00	7.69 ± 2.53	0	0	0.25 ± 0.16	0	194.59 ± 38.57
	7 days	Vehicle	140.46 ± 42.96	4.33 ± 2.56	0.75 ± 0.33	0	0.62 ± 0.31	0.10 ± 0.10	123.61 ± 28.69
		1 mg/kg MWCNT	131.73 ± 15.46	9.07 ± 3.82	0.24 ± 0.14	0	1.44 ± 0.72	0.37 ± 0.25	142.85 ± 19.49
		1 mg/kg GNS (2)	110.00 ± 10.92	3.49 ± 0.64	0	0	0.51 ± 0.34	0	114.00 ± 11.73
		1 mg/kg GNS (5)	242.84 ± 50.25	10.65 ± 4.92	0.31 ± 0.18	0.37 ± 0.37	1.34 ± 0.27	0.22 ± 0.22	255.72 ± 49.06

Notes: *$P < 0.05$; ***$P < 0.001$ compared to C57BL/6 mice injected with vehicle.
Abbreviations: MWCNT, multiwalled carbon nanotubes; GNS, graphene nanosheets.

in C57BL/6 mice demonstrated a Th2 immune response in the spleen, which consisted of increased mRNA expression of Th2 cytokines, including IL-4 and IL-33, as well as an increase in CD4$^+$ and CD8$^+$ T lymphocytes. By utilizing ST2$^{-/-}$ mice, we determined that the underlying mechanism of these CBN-induced site-specific inflammatory responses was mediated by the IL-33/ST2 axis.

The routes by which CBN are administered will likely dictate immune responses and ultimately influence the health and safety of engineered nanomaterials for biomedical applications. For example, alveolar macrophages and the pulmonary epithelium play a crucial role in immune responses induced by pulmonary exposure to CBN,[13,23–25] whereas iv administration of CBN may initiate an immune response through the activation of circulating leukocytes.[26] Our previous studies demonstrated that MWCNT instilled through oropharyngeal aspiration induces IL-33 production in the lung.[13] In the current study, however, iv injection of MWCNT leads to upregulation of IL-33 in the spleen instead of the lung. These differences in the site of IL-33 induction are likely due to differences in accumulation sites based on routes of exposure. Instillation of MWCNT-induced injury to the lung epithelium results in the release of IL-33,[13] whereas iv injection of CBN may allow for IL-33 to enter many organs through overcoming endothelial cell barriers via cellular penetration and uptake.[27] Local macrophages and the complement system are activated following the recognition of these CBN, leading to the recruitment of systemic leukocytes and facilitating inflammation at sites of CBN accumulation.[28,29] The use of iv delivery utilized in this study was selected to accurately depict the potential biomedical applications of these CBN. The dose used in our study (1 mg/kg) is within the dose range of other studies (0.02–5 mg/kg).[30–32] However, our study demonstrates that even at a relatively low dose, CBN delivery still modulates the immune system. Therefore, at higher doses, more exaggerated immune responses may occur resulting in toxicity and disease. In addition to the 1 mg/kg CBN doses, we also examined the effects induced at lower doses of CBNs including 0.01 mg/kg and 0.1 mg/kg. Neither of these lower doses administered intravenously was found to induce Th2 immune responses in the spleen or lungs (data not shown).

The translocation and biodistribution of CBN are critical factors in evaluating their potential safety in vivo. In our study, Raman spectroscopy confirmed the presence of MWCNT and GNS in both the lung and spleen following a single administration. Mice injected with GNS were found to exhibit a Th2 immune response in the lung, whereas those injected with MWCNT resulted in an immune response in

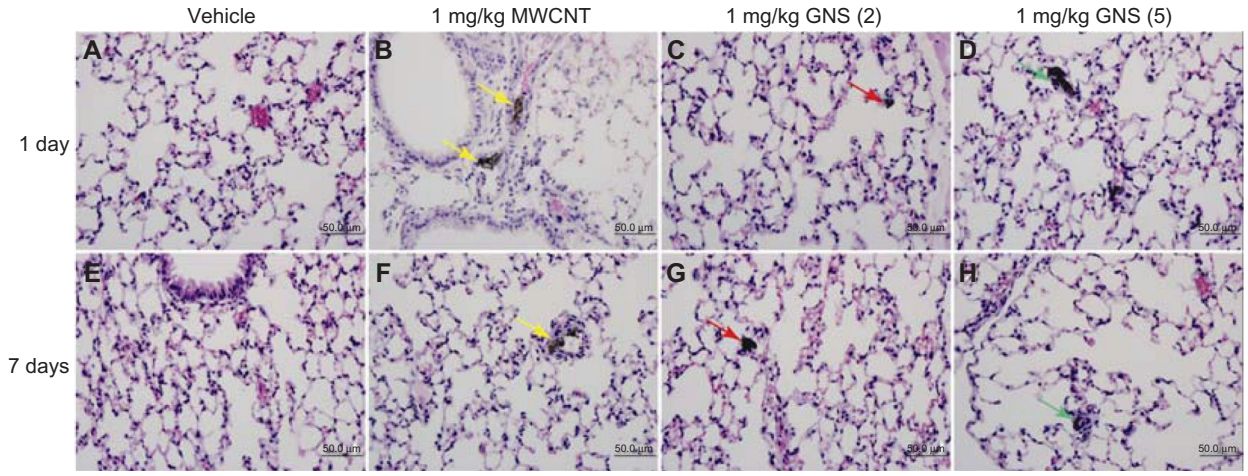

Figure 4 Histopathology in the lungs of C57BL/6 mice injected with MWCNT, GNS (2), or GNS (5). Representative histopathology of hematoxylin and eosin-stained lung sections from C57BL/6 mice at 1 or 7 days following (**A** and **E**) injection with vehicle, or (**B** and **F**) 1 mg/kg of MWCNT, (**C** and **G**) GNS (2), or (**D** and **H**) GNS (5).
Notes: Agglomerates of MWCNT within the pulmonary capillary are indicated by yellow arrows. Localization of GNS within the alveolar space is indicated by red arrows for GNS (2) and green arrows for GNS (5) at 1 or 7 days postinjection.
Abbreviations: MWCNT, multiwalled carbon nanotubes; GNS, graphene nanosheets.

the spleen. These site-specific immune responses induced by GNS and MWCNT suggest differences in the biodistribution between these two CBN. A previous study has demonstrated that iv injection of rhenium–graphene oxide into mice leads to rapid clearance of this rhenium-graphene oxide from the bloodstream and its distribution throughout the body within 48 hours, with the primary accumulation site being the lungs.[33] This is consistent with our histopathological findings demonstrating the accumulation of GNS in the alveolar spaces as early as 1 day following injection. Conversely, MWCNT have been shown to accumulate in the spleen following iv administration, irrespective of their surface characteristics.[34,35] These findings are consistent with our study, which demonstrates not only an accumulation of MWCNT in the spleen, but also an induction of immune responses in the spleen after exposure. Overall, our findings indicate differences in organ distribution for the two types of CBN and thereby differences in sites of inflammation. These different patterns of biodistribution may be useful in developing drug delivery systems for specific organs. Further studies assessing the biodistribution of CBN are needed using fluorescence- or radioisotope-labeled nanomaterials to quantify nanomaterials in each organ.

The physicochemical properties of CBN, such as shape, size, surface charge, and the addition of functional groups, can have a dramatic impact on their biodistribution in vivo.[36,37] Compositionally, GNS and MWCNT are similar and consist primarily of carbon. However, GNS and MWCNT are dramatically different in regard to shape, surface area, and the presence of metal catalysts, which may influence their respective biodistribution. A previous study comparing GNS with SWCNT has demonstrated differences in neuronal PC12 cell cytotoxicity possibly due to their shape and/or state of agglomeration.[38] Similarly, in our study, differences in site-specific inflammatory responses are likely explained by the shape and agglomeration state of these CBN and their biological interactions with the endothelial barrier of the circulatory system. Our lung histology results showed that some agglomerated MWCNT accumulated in the pulmonary capillary by 1 day, but did not reach the alveolar spaces, while GNS clearly reached the alveolar spaces within 1 day following injection. GNS, with their flat shape, appear to readily penetrate the endothelial barrier of the pulmonary capillary. However, MWCNT, with their tubular shape agglomerate easily and may not readily penetrate the endothelial barrier, inhibiting their entrance into the lung. An accumulating amount of evidence has suggested that different CBN have different renal clearance speed and urinary excretion rates due to their physicochemical properties.[39] Therefore, further studies are needed to illustrate the efficiency of renal clearance and urinary excretion of these CBN. The different sizes of GNS produced different responses in the lung, with smaller sized GNS being more potent at inducing a Th2 immune response. These size-dependent differences in the immune response of GNS might be due to differences in internalization by phagocytes, since the efficient internalization of nanomaterials by phagocytes is reported to be partly size dependent.[40]

Previous studies in our laboratory and others have demonstrated that pulmonary exposure to MWCNT induces

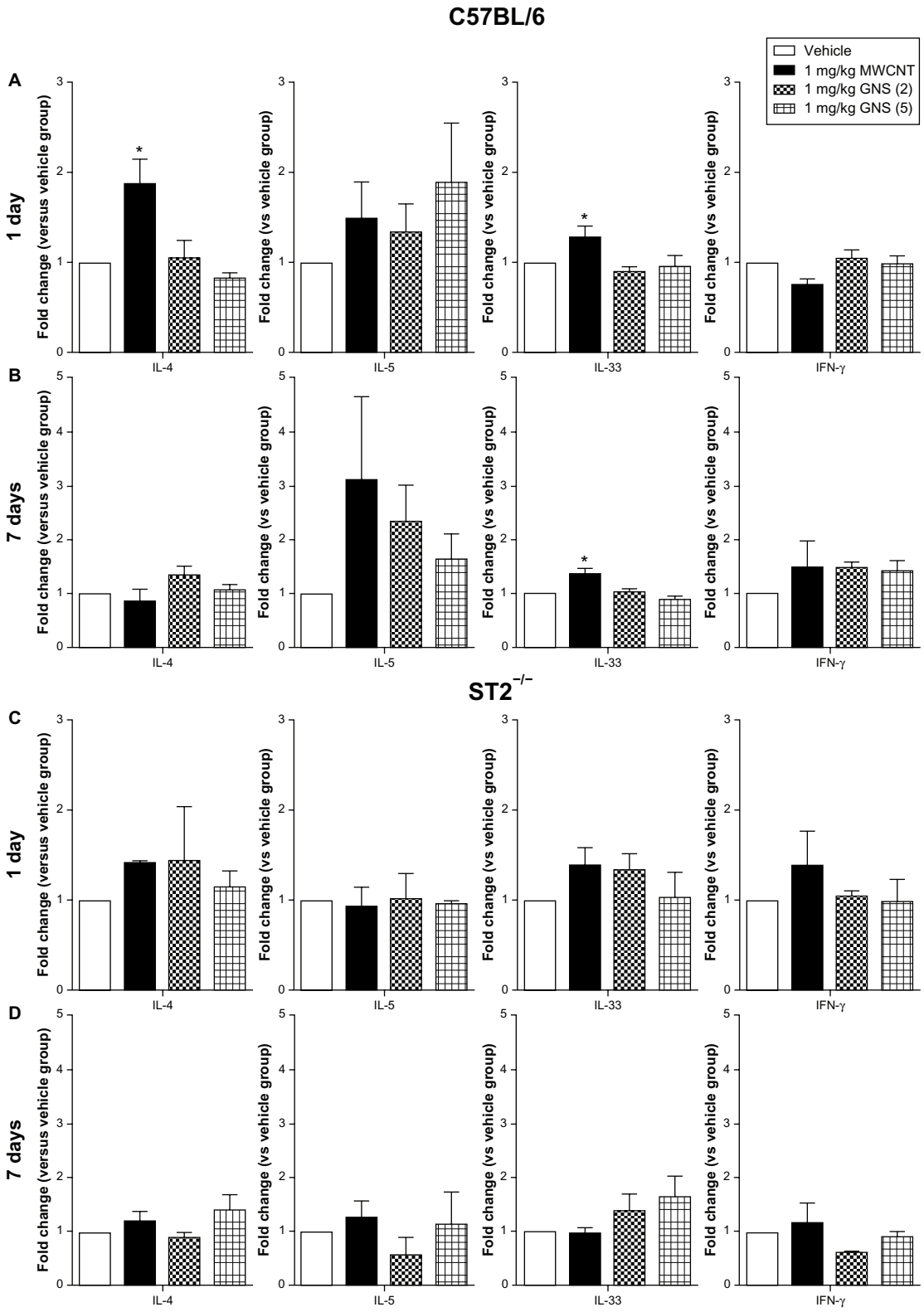

Figure 5 mRNA expression of Th1/Th2 cytokines in spleens of C57BL/6 and ST2$^{-/-}$ mice 1 or 7 days following intravenous injection with MWCNT, GNS (2), or GNS (5). Real-time PCR analysis for mRNA expression of IL-4, IL-5, IL-33, and IFN-γ was performed in spleen tissue from vehicle or 1 mg/kg of MWCNT, GNS (2), or GNS (5) injected (**A** and **B**) C57BL/6 and (**C** and **D**) ST2$^{-/-}$ (**C** and **D**) mice at (**A** and **C**) 1 day and (**B** and **D**) 7 days postinjection.

Notes: All values are expressed as the mean ± SEM (n = 4 per group). *$P < 0.05$ compared to strain-matched vehicle control.

Abbreviations: mRNA, messenger ribonucleic acid; MWCNT, multiwalled carbon nanotubes; GNS, graphene nanosheets; PCR, polymerase chain reaction; IL, interleukin; IFN, interferon; SEM, standard error of the mean; n, number.

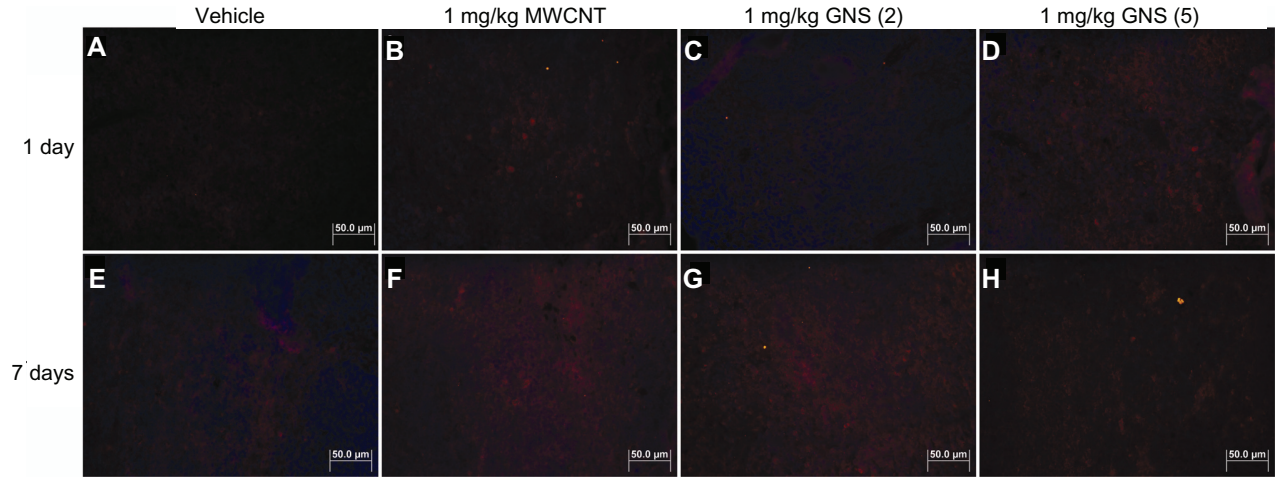

Figure 6 IL-33 protein expression in spleens of C57BL/6 mice 1 or 7 days following intravenous injection with MWCNT, GNS (2), or GNS (5).
Note: Representative immunofluorescence images of IL-33 protein expression (red) in spleen from C57BL/6 mice at 1 or 7 days following injection with (**A** and **E**) vehicle or (**B** and **F**) 1 mg/kg of MWCNT, (**C** and **G**) GNS (2), or (**D** and **H**) GNS (5).
Abbreviations: IL, interleukin; MWCNT, multiwalled carbon nanotubes; GNS, graphene nanosheets.

IL-33 as an alarmin to activate the immune system and may be a major mechanism responsible for MWCNT-induced cardiopulmonary toxicity.[12,13,25,41] To date, however, there have been no studies describing the effects of CBN through iv injection with regards to IL-33 production. Our results demonstrate that injection of GNS caused a marked increase in IL-33 production in the lung, while MWCNT injection resulted in elevated IL-33 mRNA expression within the spleen. IL-33 has been found to be constitutively expressed in the epithelial cells of bronchus and small airways of both mice and humans with allergic asthma,[42–44] as well as in CBN-induced pulmonary toxicity.[12,13,25] The alarmin IL-33 released from damaged endothelial or epithelial cells may induce the activation of the inflammasome and promote the release of cytokines (such as IL-5 and IL-13) from different cell types including macrophages, mast cells, basophils, and T-helper cells.[14–16] Our data supports previous IL-33 observations by showing that GNS induce transient increases in IL-33 production in the lung,[13] which consequently promotes the release of IL-5 and IL-13 1 day following iv administration, thereby leading to inflammatory cell recruitment.

The spleen is the major organ of the reticuloendothelial system where accumulation of MWCNT has been shown to occur following iv administration, irrespective of surface characteristics including hydrophilicity, hydrophobicity, and surface charge.[34,35] Our results established that iv injection of MWCNT leads to the upregulation of IL-33 mRNA in the spleen of mice and continues to be elevated through 7 days. While the cellular source of IL-33 remains unknown following MWCNT delivery, it has been reported that stromal cells are a source of IL-33 mRNA and of protein expression in mouse spleen.[45] Meanwhile, IL-4 mRNA expression was found to be increased in the spleen 1 day following injection of MWCNT. This increase in IL-4 mRNA expression might be due to the increase in IL-33, since a previous study has shown that IL-33 promotes antigen-stimulated Th2 cells to increase production of IL-4.[46]

Although ST2 has been predominantly detected on $CD4^+$ Th2 cells,[47] recent studies have found that ST2 is also highly expressed on $CD8^+$ T cells.[19,48] ST2 plays an auxiliary role in the differentiation of $CD4^+$ Th2 cells, but a critical role in the development of an effective Th2 response.[49] Signaling through ST2 has been found to increase transcription of a variety of genes in $CD8^+$ effector T-cells, including those associated with differentiation, proliferation, migration, and adhesion.[48] In addition, IL-33 has been found to be expressed in nonhematopoietic cells within the splenic T-cell zone, where the initiation and expansion of T-cell responses is known to occur.[48] Our study shows significant increases in both $CD4^+$ and $CD8^+$ T-cells 1 day following injection of MWCNT, as well as the continued elevation of $CD4^+$ T-cells through 7 days. In contrast, when MWCNT were injected in mice lacking the ST2 receptor, there was not an increase in the $CD4^+$ or $CD8^+$ T cell populations in the spleen. Maintaining the proper number and proportion of $CD4^+$ and $CD8^+$ T-cells is essential for optimal host defense.[50] Therefore, disturbing this balance following CBN exposure could lead to adverse effects on host defense or allergic diseases. These findings

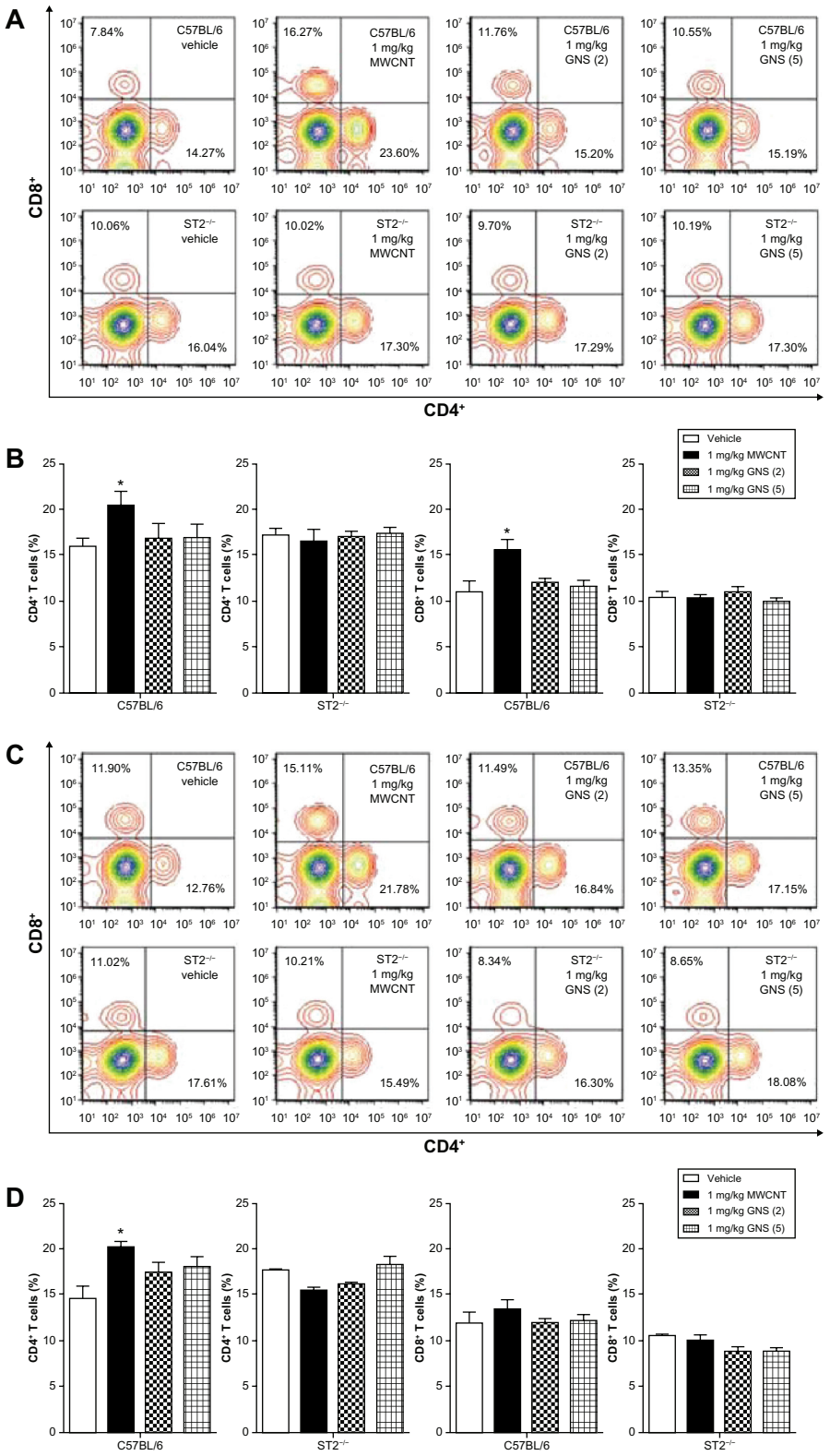

Figure 7 CD4 and CD8 expression on splenocytes of C57BL/6 and ST2$^{-/-}$ mice 1 or 7 days following intravenous injection with MWCNT, GNS (2), or GNS (5). Surface expression of CD4 and CD8 on splenocytes was analyzed by flow cytometry at (**A** and **B**) 1 day or (**C** and **D**) 7 days following injection with vehicle or 1 mg/kg of MWCNT, GNS (2), or GNS (5) in C57BL/6 and ST2$^{-/-}$ mice. (**A** and **C**) Each multicolor contour plot is a representative of 4–8 independent mice at 1 or 7 days postinjection. (**B** and **D**) Changes in CD4^{+} and CD8^{+} T lymphocytes (%) in C57BL/6 and ST2$^{-/-}$ mouse spleen at 1 or 7 days following intravenous injection.

Notes: Values are expressed as the mean ± SEM (n = 4–8 per group). *$P < 0.05$ compared to strain-matched vehicle control.

Abbreviations: CD, cell differentiation; MWCNT, multiwalled carbon nanotubes; GNS, graphene nanosheets; SEM, standard error of the mean; n, number.

Table 3 Effect of MWCNT and GNS on splenocyte population in C57BL/6 and ST2$^{-/-}$ mice at 1 day or 7 days following intravenous injection

Strain	Time point	Treatment	Lymphocytes (×10^6 cells/mL)	Total cells (×10^6 cells/mL)
C57BL/6	1 day	Vehicle	11.32 ± 1.16	13.31 ± 1.31
		1 mg/kg MWCNT	12.09 ± 1.29	14.66 ± 1.48
		1 mg/kg GNS (2)	12.96 ± 1.55	16.73 ± 1.74
		1 mg/kg GNS (5)	16.77 ± 1.49	22.53 ± 1.49*
	7 days	Vehicle	10.47 ± 0.91	13.13 ± 0.93
		1 mg/kg MWCNT	10.92 ± 0.53	13.91 ± 0.54
		1 mg/kg GNS (2)	12.85 ± 0.24	16.68 ± 0.58
		1 mg/kg GNS (5)	11.33 ± 1.41	14.71 ± 1.08
ST2$^{-/-}$	1 day	Vehicle	15.52 ± 0.98	17.41 ± 1.07
		1 mg/kg MWCNT	13.53 ± 2.20	15.23 ± 2.34
		1 mg/kg GNS (2)	13.85 ± 1.54	15.73 ± 1.39
		1 mg/kg GNS (5)	16.03 ± 2.80	18.14 ± 3.36
	7 days	Vehicle	14.48 ± 2.20	15.68 ± 2.37
		1 mg/kg MWCNT	15.13 ± 2.17	17.45 ± 2.14
		1 mg/kg GNS (2)	13.47 ± 1.61	14.61 ± 1.58
		1 mg/kg GNS (5)	15.25 ± 2.09	16.87 ± 2.03

Note: *$P < 0.05$ compared to C57BL/6 mice injected with vehicle.
Abbreviations: MWCNT, multiwalled carbon nanotubes; GNS, graphene nanosheets.

clearly point to an important role for IL-33 and its receptor ST2 in the proliferation of CD4$^+$ and CD8$^+$ T-cells following iv administration of MWCNT. Meanwhile, these results also support activation of the ST2 receptor as a mechanism for CBN-induced systemic toxicity.

Conclusion

The unique properties of CBN – including but not limited to size, covalent bonding to different drugs, and high loading capacity – has prompted their use in nanomedicine.[51,52] However, the safety of CBN as drug carriers remains a concern. In order for CBN to be used safely in drug delivery systems, we have to understand their interactions with the immune system. In the current study, we have demonstrated that iv injection of CBN results in site-specific immune responses with polarization towards a Th2 response in the lung and spleen. Furthermore, we validated that these CD4$^+$ Th2 immune responses induced by CBN were mediated by the IL-33/ST2 axis. By establishing the IL-33/ST2 axis as a potential mechanism of CBN-induced immunotoxicity, IL-33 may prove to be a useful screening tool to assess the safety of nanomedicines. A shift in the Th1/Th2 balance by CBN could have profound effects on both host defense and the exacerbation of allergic diseases such as asthma and anaphylaxis. These different immunotoxicologic effects induced by iv administration of GNS and MWCNT are likely due to their varied physicochemical properties. Further modification of these CBN may be necessary to decrease the potential immunotoxicity related to iv delivery and to ensure their safety for use in nanomedicines.

Acknowledgments

This work was supported by the National Institute of Environmental Health Sciences RO1 ES 019311.

Disclosure

The authors report no conflicts of interest in this work.

References

1. Alexis F, Rhee JW, Richie JP, Radovic-Moreno AF, Langer R, Farokhzad OC. New frontiers in nanotechnology for cancer treatment. *Urol Oncol*. 2007;26(1):74–85.
2. Ji SR, Liu C, Zhang B, et al. Carbon nanotubes in cancer diagnosis and therapy. *Biochim Biophys Acta*. 2010;1806(1):29–35.
3. Chang C. The immune effects of naturally occurring and synthetic nanoparticles. *J Autoimmun*. 2010;34(3):J234–J246.
4. Grimm J, Scheinberg DA. Will nanotechnology influence targeted cancer therapy? *Semin. Radiat Oncol*. 2011;21(2):80–87.
5. Liu Z, Robinson JT, Tabakman SM, Yang K, Dai H. Carbon materials for drug delivery and cancer therapy. *Mater Today*. 2011;14(7–8):316–323.
6. Misra R, Acharya S, Sahoo SK. Cancer nanotechnology: application of nanotechnology in cancer therapy. *Drug Discov Today*. 2010;15(19–20):842–850.
7. Zhang Y, Bai Y, Yan B. Functionalized carbon nanotubes for potential medicinal applications. *Drug Discov Today*. 2010;15(11–12):428–435.
8. Nygaard UC, Hansen JS, Samuelsen M, Alberg T, Marioara CD, Løvik M. Single-walled and multi-walled carbon nanotubes promote allergic immune responses in mice. *Toxicol Sci*. 2009;109(1):113–123.
9. Mitchell LA, Lauer FT, Burchiel SW, McDonald JD. Mechanisms for how inhaled multiwalled carbon nanotubes suppress systemic immune function in mice. *Nat Nanotechnol*. 2009;4(7):451–456.
10. Yamaguchi A, Fujitani T, Ohyama K, et al. Effects of sustained stimulation with multi-wall carbon nanotubes on immune and inflammatory responses in mice. *J Toxicol Sci*. 2012;37(1):177–189.

11. Andersen AJ, Wibroe PP, Moghimi SM. Perspectives on carbon nanotube-mediated adverse immune effects. *Adv Drug Deliv Rev*. 2012;64(15):1700–1705.
12. Wang X, Katwa P, Podila R, et al. Multi-walled carbon nanotube instillation impairs pulmonary function in C57BL/6 mice. *Part Fibre Toxicol*. 2011;8:24.
13. Katwa P, Wang X, Urankar RN, et al. A carbon nanotube toxicity paradigm driven by mast cells and the IL-33/ST2 axis. *Small*. 2012;8(18): 2904–2912.
14. Schmitz J, Owyang A, Oldham E, et al. IL-33, an interleukin-1-like cytokine that signals via the IL-1 receptor-related protein ST2 and induces T helper type 2-associated cytokines. *Immunity*. 2005;23(5): 479–490.
15. Lloyd CM. IL-33 family members and asthma – bridging innate and adaptive immune responses. *Curr Opin Immunol*. 2010;22(6):800–806.
16. Oboki K, Ohno T, Kajiwara N, Saito H, Nakae S. IL-33 and IL-33 receptors in host defense and diseases. *Allergol Int*. 2010;59(2):143–160.
17. Liew FY, Pitman NI, McInnes IB. Disease-associated functions of IL-33: the new kid in the IL-1 family. *Nat Rev Immunol*. 2010;10(2): 103–110.
18. Hayakawa H, Hayakawa M, Kume A, Tominaga S. Soluble ST2 blocks interleukin-33 signaling in allergic airway inflammation. *J Biol Chem*. 2007;282(36):26369–26380.
19. Yang Q, Li G, Zhu Y, et al. IL-33 synergizes with TCR and IL-12 signaling to promote the effector function of CD8+ T cells. *Eur J Immunol*. 2011;41(11):3351–3360.
20. Bihari P, Vippola M, Schultes S, et al. Optimized dispersion of nanoparticles for biological in vitro and in vivo studies. *Part Fibre Toxicol*. 2008;5:14.
21. Moore TL, Pitzer JE, Podila R, et al. Multifunctional Polymer-Coated Carbon Nanotubes for Safe Drug Delivery. *Particle and Particle Systems Characterization*. 2013;30(4):365–373.
22. Wang H, Yang ST, Cao A, Liu Y. Quantification of carbon nanomaterials in vivo. *Acc Chem Res*. Epub October 4, 2012.
23. Mercer RR, Hubbs AF, Scabilloni JF, et al. Pulmonary fibrotic response to aspiration of multi-walled carbon nanotubes. *Part Fibre Toxicol*. 2011;8:21.
24. Porter DW, Hubbs AF, Chen BT, et al. Acute pulmonary dose-responses to inhaled multi-walled carbon nanotubes. *Nanotoxicology*. Epub September 13, 2012.
25. Beamer CA, Girtsman TA, Seaver BP, et al. IL-33 mediates multi-walled carbon nanotube (MWCNT)-induced airway hyper-reactivity via the mobilization of innate helper cells in the lung. *Nanotoxicology*. Epub June 29, 2012.
26. Medepalli K, Alphenaar B, Raj A, Sethu P. Evaluation of the direct and indirect response of blood leukocytes to carbon nanotubes (CNTs). *Nanomedicine*. 2011;7(6):983–991.
27. Albini A, Mussi V, Parodi A, et al. Interactions of single-wall carbon nanotubes with endothelial cells. *Nanomedicine*. 2010;6(2):277–288.
28. Murphy FA, Schinwald A, Poland CA, Donaldson K. The mechanism of pleural inflammation by long carbon nanotubes: interaction of long fibres with macrophages stimulates them to amplify pro-inflammatory responses in mesothelial cells. *Part Fibre Toxicol*. 2012;9:8.
29. Rybak-Smith MJ, Sim RB. Complement activation by carbon nanotubes. *Adv Drug Deliv Rev*. 2011;63(12):1031–1041.
30. Bai Y, Zhang Y, Zhang J, et al. Repeated administrations of carbon nanotubes in male mice cause reversible testis damage without affecting fertility. *Nat Nanotechnol*. 2010;5(9):683–689.
31. Cherukuri P, Gannon CJ, Leeuw TK, et al. Mammalian pharmacokinetics of carbon nanotubes using intrinsic near-infrared fluorescence. *Proc Natl Acad Sci U S A*. 2006;103(50):18882–18886.
32. Patlolla AK, Hussain SM, Schlager JJ, Patlolla S, Tchounwou PB. Comparative study of the clastogenicity of functionalized and non-functionalized multiwalled carbon nanotubes in bone marrow cells of Swiss-Webster mice. *Environ Toxicol*. 2010;25(6):608–621.
33. Zhang X, Yin J, Peng C, et al. Distribution and biocompatibility studies of graphene oxide in mice after intravenous administration. *Carbon*. 2011;49(3):986–995.
34. Jain S, Thakare VS, Das M, et al. Toxicity of multiwalled carbon nanotubes with end defects critically depends on their functionalization density. *Chem Res Toxicol*. 2011;24(11):2028–2039.
35. Wu H, Liu G, Zhuang Y, et al. The behavior after intravenous injection in mice of multiwalled carbon nanotube/Fe3O4 hybrid MRI contrast agents. *Biomaterials*. 2011;32(21):4867–4876.
36. Murphy FA, Poland CA, Duffin R, Donaldson K. Length-dependent pleural inflammation and parietal pleural responses after deposition of carbon nanotubes in the pulmonary airspaces of mice. *Nanotoxicology*. Epub August 21, 2012.
37. Li M, Panagi Z, Avgoustakis K, Reineke J. Physiologically based pharmacokinetic modeling of PLGA nanoparticles with varied mPEG content. *Int J Nanomedicine*. 2012;7:1345–1356.
38. Zhang Y, Ali SF, Dervishi E, et al. Cytotoxicity effects of graphene and single-wall carbon nanotubes in neural phaeochromocytoma-derived PC12 cells. *ACS Nano*. 2010;4(6):3181–3186.
39. Lacerda L, Herrero MA, Venner K, Bianco A, Prato M, Kostarelos K. Carbon-nanotube shape and individualization critical for renal excretion. *Small*. 2008;4(8):1130–1132.
40. Wang X, Reece SP, Brown JM. Immunotoxicological impact of engineered nanomaterial exposure: mechanisms of immune cell modulation. *Toxicol Mech Methods*. 2013;23(3):168–177.
41. Inoue K, Koike E, Yanagisawa R, Hirano S, Nishikawa M, Takano H. Effects of multi-walled carbon nanotubes on a murine allergic airway inflammation model. *Toxicol Appl Pharmacol*. 2009;237(3): 306–316.
42. Willart MA, Deswarte K, Pouliot P, et al. Interleukin-1α controls allergic sensitization to inhaled house dust mite via the epithelial release of GM-CSF and IL-33. *J Exp Med*. 2012;209(8):1505–1517.
43. Hammad H, Chieppa M, Perros F, Willart MA, Germain RN, Lambrecht BN. House dust mite allergen induces asthma via Toll-like receptor 4 triggering of airway structural cells. *Nat Med*. 2009;15(4): 410–416.
44. Wills-Karp M, Rani R, Dienger K, et al. Trefoil factor 2 rapidly induces interleukin 33 to promote type 2 immunity during allergic asthma and hookworm infection. *J Exp Med*. 2012;209(3):607–622.
45. Talabot-Ayer D, Calo N, Vigne S, Lamacchia C, Gabay C, Palmer G. The mouse interleukin (Il)33 gene is expressed in a cell type- and stimulus-dependent manner from two alternative promoters. *J Leukoc Biol*. 2012;91(1):119–125.
46. Matsuba-Kitamura S, Yoshimoto T, Yasuda K, et al. Contribution of IL-33 to induction and augmentation of experimental allergic conjunctivitis. *Int Immunol*. 2010;22(6):479–489.
47. Meisel C, Bonhagen K, Löhning M, et al. Regulation and function of T1/ST2 expression on CD4+ T cells: induction of type 2 cytokine production by T1/ST2 cross-linking. *J Immunol*. 2001;166(5):3143–3150.
48. Bonilla WV, Fröhlich A, Senn K, et al. The alarmin interleukin-33 drives protective antiviral CD8+ T cell responses. *Science*. 2012;335(6071): 984–989.
49. Trajkovic V, Sweet MJ, Xu D. T1/ST2 – an IL-1 receptor-like modulator of immune responses. *Cytokine Growth Factor Rev*. 2004;15(2–3): 87–95.
50. Germain RN. T-cell development and the CD4-CD8 lineage decision. *Nat Rev Immunol*. 2002;2(5):309–322.
51. Mocan T, Iancu C. Effective colon cancer prophylaxis in mice using embryonic stem cells and carbon nanotubes. *Int J Nanomedicine*. 2011; 6:1945–1954.
52. Madani SY, Naderi N, Dissanayake O, Tan A, Seifalian AM. A new era of cancer treatment: carbon nanotubes as drug delivery tools. *Int J Nanomedicine*. 2011;6:2963–2979.

Supplementary materials

Table S1 Sizes and numbers of CBN agglomerates in the lungs

Treatment	Time point	L (μm)	P (μm)	Agglomerates per slide (N)
1 mg/kg MWCNT	1 day	63.58 ± 15.76	34.19 ± 3.46	12.79 ± 3.66
	7 days	36.29 ± 2.62	25.18 ± 1.45	8.95 ± 3.13
1 mg/kg GNS (2)	1 day	27.10 ± 3.18	20.39 ± 2.89	8.79 ± 1.54
	7 days	17.66 ± 1.41	13.88 ± 1.45	6.08 ± 0.71
1 mg/kg GNS (5)	1 day	20.10 ± 1.30	14.48 ± 0.92	4.98 ± 0.77
	7 days	19.4 ± 1.47	14.11 ± 1.03	10.74 ± 2.07

Abbreviations: CBN, carbon-based nanomaterials; L, longest axis; P, perpendicular axis with the longest axis; N, number; MWCNT, multiwalled carbon nanotubes; GNS, graphene nanosheets.

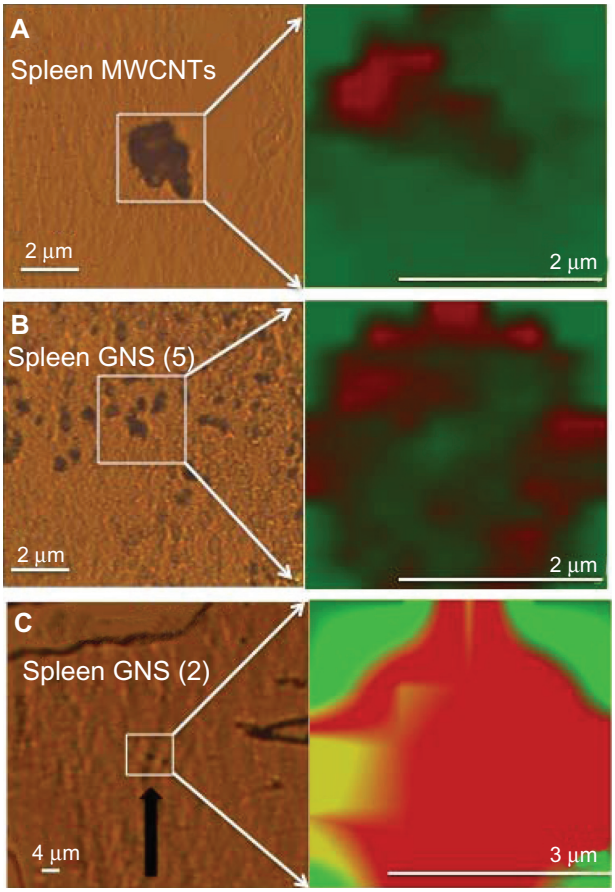

Figure S1 Optical microscope images and the corresponding micro-Raman maps for spleen sections exposed to MWCNTs and GNS. Optical microscope images and the corresponding micro-Raman maps for spleen sections exposed (**A**) MWCNTs, (**B**) GNS (5), and (**C**) GNS (2).
Note: In the Raman maps, the red and green colored areas indicate high and no intensity for G-band respectively.
Abbreviations: MWCNT, multiwalled carbon nanotubes; GNS, graphene nanosheets.

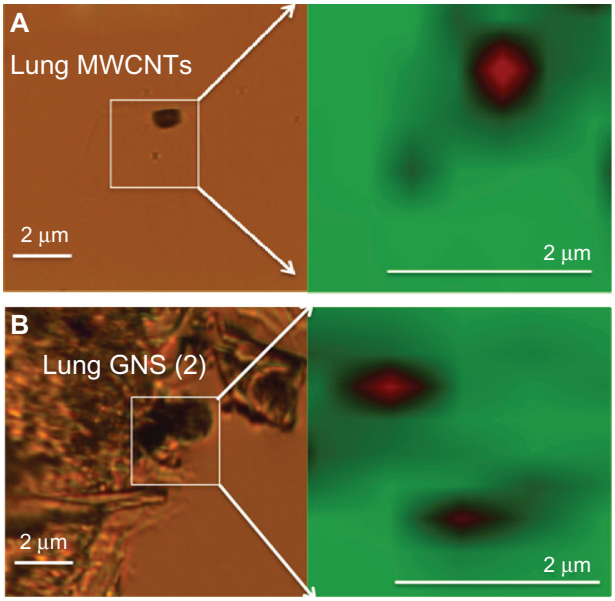

Figure S2 Optical microscope images and the corresponding micro-Raman maps for lung sections exposed to MWCNTs and GNS. Optical microscope images and the corresponding micro-Raman maps for lung sections exposed to (**A**) MWCNTs and (**B**) GNS.
Note: In the Raman maps, the red and green colored areas indicate high and no intensity for G-band, respectively.
Abbreviations: MWCNT, multiwalled carbon nanotubes; GNS, graphene nanosheets.

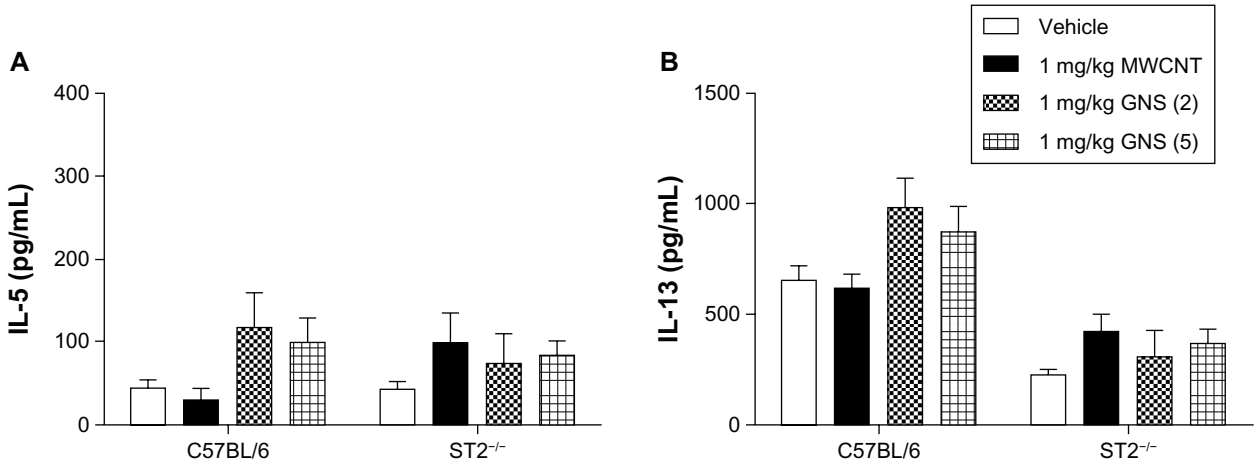

Figure S3 Production of the Th2 cytokines, IL-5 and IL-13, were measured by ELISA in BALF from the lungs of C57BL/6 and ST2$^{-/-}$ mice at 7 days following injection with vehicle or 1 mg/kg of MWCNT, GNS (2), or GNS (5). Production of the Th2 cytokines, (**A**) IL-5 and (**B**) IL-13, were measured by ELISA in BALF from the lungs of C57BL/6 and ST2$^{-/-}$ mice at 7 days following injection with vehicle or 1 mg/kg of MWCNT, GNS (2), or GNS (5).
Note: Values are expressed as the mean ± SEM (n = 4–8 per group).
Abbreviations: IL, interleukin; ELISA, enzyme-linked immunosorbent assay; BALF, bronchoalveolar lavage fluid; MWCNT, multiwalled carbon nanotubes; GNS, graphene nanosheets; SEM, standard error of the mean.

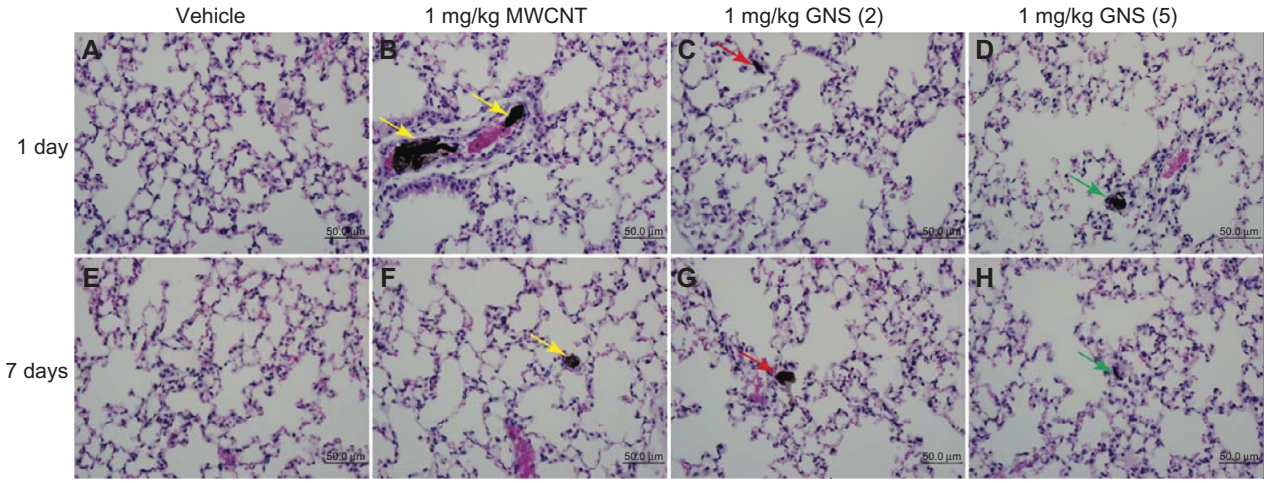

Figure S4 Representative histopathology of hematoxylin and eosin-stained lung sections from ST2$^{-/-}$ mice at 1 or 7 days following injection with vehicle or 1 mg/kg MWCNT, GNS (2), or GNS (5). Representative histopathology of hematoxylin and eosin stained lung sections from ST2$^{-/-}$ mice at 1 or 7 days following injection with (**A** and **E**) vehicle or (**B** and **F**) 1 mg/kg of MWCNT, (**C** and **G**) GNS (2), or (**D** and **H**) GNS (5).
Notes: Agglomerates of MWCNT within pulmonary capillaries are indicated by yellow arrows. Localization of GNS within the alveolar space is indicated by red arrows for GNS (2) and green arrows for GNS (5) at 1 or 7 days postinjection.
Abbreviations: MWCNT, multiwalled carbon nanotubes; GNS, graphene nanosheets.